Prediction of Separated Flows with a New Backflow Turbulence Model

Uriel C. Goldberg* and Sukumar R. Chakravarthy*
Rockwell International Science Center, Thousand Oaks, California

A recently introduced[1] backflow turbulence model for separated flows has been used to calculate the reattaching flow over a backward facing step and the shock-induced separation over an axisymmetric bump. Results are compared with experimental data and with calculations using the *k–e* turbulence model and the Johnson-King model. It is concluded that the new backflow turbulence model performs as well as the Johnson-King model and better than the *k–e* model.

Nomenclature

c = bump length
C_p = pressure coefficient, $2(p-p_\infty)/\rho_\infty U_\infty^2$
H = step height
k = kinetic energy of turbulence
n = coordinate locally normal to the wall
p = pressure
s = coordinate locally parallel to the wall
U = mean streamwise velocity
u_s = velocity scale for separated flows
U_t = locally tangential mean velocity component
ϵ = isotropic part of turbulence energy dissipation
ν = kinematic molecular viscosity
ν_t = kinematic eddy viscosity
ρ = density
τ = shear stress

Subscripts

b = evaluated at the backflow edge
v = evaluated at a location eleven viscous lengths outside the backflow edge
w = evaluated at the wall
∞ = upstream conditions

Introduction

THE reattachment of a turbulent shear layer has been regarded as a crucial test for the performance of turbulence models. Recently, Driver and Seegmiller[1] reported experimental and computational results for turbulent flow over a backward-facing step. The calculations, performed by Sindir,[2] used the k–ϵ model and an algebraic Reynolds stress model (ARSM), alternatively. Both models caused premature reattachment prediction, and a modified ϵ equation was necessary in order to improve agreement between the calculations using the ARSM and the data. The same modified ϵ equation did not improve predictional quality when used with the k–ϵ model. This situation renders these models less universal than they are thought to be, a rather disturbing fact to users.

Another problematic area for current turbulence models is shock-induced separation in transonic flows. As reported in Ref. 3, while the k–ϵ model with a near-wall treatment performs well for attached flows, this is no longer the case for separated flow regions. Clearly, the mechanisms of turbulence within these regions are not conveyed by either the k–ϵ model or most other currently used turbulence models.

In a previous paper,[4] a new algebraic k–ϵ turbulence model was used successfully to predict shock-induced separated flows at transonic and supersonic Mach numbers. In the present work, the very same backflow model is employed in calculating the incompressible reattaching flow reported in Ref. 1 and the separated flow over an axisymmetric bump at $M_\infty = 0.875$.[5] Results are compared both with experimental data and with calculations using the original k–ϵ model.[1-3] For the latter problem, comparisons are also made with the Johnson-King[6] model.

Highlights of the Backflow Model

As pointed out in Ref. 7, the new backflow turbulence model is based on the following experimental observations of separated flows: 1) backflows are governed by large-scale outer-region eddies, whose influence increases as the backflows develop downstream of detachment; 2) initial conditions, such as the upstream boundary layer, have little influence on the flow structure within separated flow regions; 3) the Reynolds stresses within backflow regions are a product of the turbulence structure, not of the local mean velocity gradients; 4) turbulence energy production is negligible within backflow regions, thus dissipation balances outer region turbulence energy influx by diffusion; 5) the local maximum Reynolds stress, occurring in the outer portion of a detached shear layer, provides the proper velocity scale for separated flows; 6) separating shear layers progressively behave more like free shear mixing layers; and 7) the part of a backflow adjacent to the wall has little Reynolds stress effects.

Observations 1 and 2 suggest that, once a backflow is formed, it tends to retain its turbulence structure, and the persistence of the large-scale outer eddies shields this structure from both upstream and downstream influences. This would bring the backflow to a state of local dynamic equilibrium. It is this physical picture that suggests the formulation of an equilibrium backflow turbulence model, in which turbulence quantities are expressed algebraically within the separation bubble. Observations 3, 4, and 5 provide a clear indication that the Law-of-the-Wall is ruled out for separated flow regions, and, thus, any backflow model formulation should exclude the usage of classical wall functions. Lastly, observations 6 and 7 suggest a strong wake-like behavior of the flow within separation bubbles. That this behavior extends to the turbulence structure is apparent from measurements of kinetic energy within such regions. Figure 2 of Ref. 7 provides a typical example for this behavior and actually suggests a Gaussian variation of k normal to walls within backflows. This prompts the idea of using k and ϵ as the basic variables for the backflow model. This approach has the additional advantage of enabling the interface with a

Received Nov. 19, 1986; revision received June 23, 1987.

*Member of Technical Staff. Member AIAA.

wide variety of outer-region turbulence models that may not be formulated in terms of eddy viscosity, such as Reynolds stress models that use k and ϵ as auxiliary variables.

The new backflow model, therefore, prescribes turbulence kinetic energy k and its dissipation ϵ analytically inside backflow regions, with a Gaussian variation of k assumed normal to walls. The local length scale of turbulence is proportional to the thickness of the backflow, as defined by a line located just outside the backflow region, shown in Fig. 1. The velocity scale is related to the local maximum Reynolds stress, which typically occurs well outside the bubble, in the outer region. This scale must be supplied by an outer-region turbulence model.

The eddy viscosity formulation of the backflow model is given in the Appendix. This simple formula is used to supply eddy viscosity for the Reynolds-averaged equations when the calculations are performed inside backflows. Outside, another turbulence model (e.g., Baldwin-Lomax or k–ϵ) provides the values of eddy viscosity. To date, only the Baldwin-Lomax model has been used in the outer region. In order to mimic the influence of the large eddies residing outside separation zones, the following ad hoc averaging procedure was found adequate when switching from the backflow model to the outer one: outside backflows, normal to walls, the eddy viscosity is taken to be the average of those supplied by the two models, with the backflow model used in its high Reynolds number outer form (see Appendix). Downstream of reattachment (if such exists), the history effect of the large eddies is taken into account by averaging the locally predicted eddy viscosity level with the one given by the backflow model at the backflow location where the skin friction attains its maximum negative value. It is expected that the latter averaging procedure will be eliminated once a dynamic (e.g., 1- or 2-equation) turbulence model is used beyond backflows, since such a model has a built-in history effect.

Further details about the new model, as well as mathematical derivations, are given in Ref. 7. As seen in Figs. 2 and 3 of Ref. 7, the range of validity of the backflow model seems to extend well beyond the backflow, deep into the outer region. This prompts the suggestion that using the outer formula for eddy viscosity (see Appendix) by itself or averaged with the values of eddy viscosity provided by the outer (Baldwin-Lomax) model, retains enough physics to enable adequate prediction of the outer-region eddy viscosity field and may obviate the need to use a dynamic outer model—at least for a wide variety of separated flow situations where the bubbles are not large enough to significantly after the inviscid farfield.

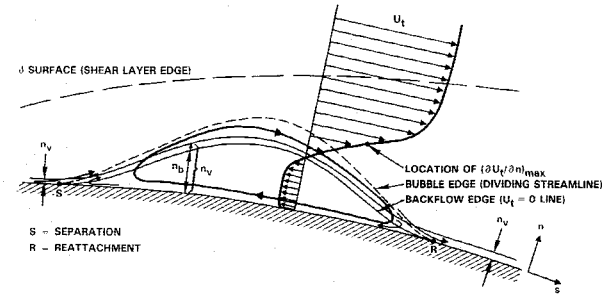

Fig. 1 Schematic view of a separated flow bubble and basic nomenclature.

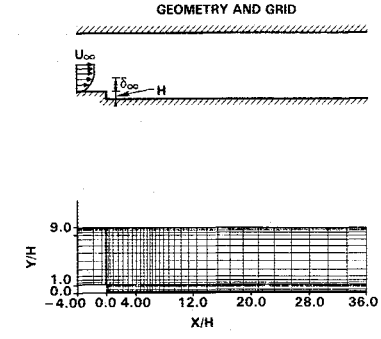

Fig. 2 Two-zone computational grid and geometry.

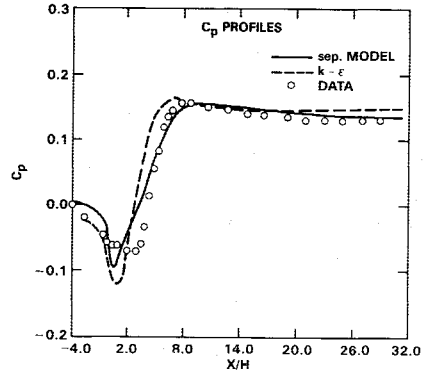

Fig. 3 Step-side pressure distribution.

Computational Results

The algebraic k–ϵ backflow model, in conjunction with the Baldwin-Lomax model, has been incorporated into a finite volume time-marching zonal Navier-Stokes code,[8,9] featuring an implicit upwind-biased scheme, approximate factorization, and total variation diminishing discretization for high accuracy. The Baldwin-Lomax model was used to compute eddy viscosity outside backflow regions, while the new model provided eddy viscosity within these regions. This code was used to calculate the following cases: 1) the backward-facing step case reported in Ref. 1, with an inflow Mach number of 0.128 and a Reynolds number of 31,250 based on inflow conditions and the step height as a reference length; 2) the axisymmetric bump reported in Ref. 5 and $M_\infty = 0.875$ and $\mathrm{Re}_\infty = 13.6 \times 10^6$m.

Case 1

Figure 2 shows the geometry and the two-zone computational grid, with a 42×22 mesh used in the subdomain above the step and a 36×20 mesh used in the subdomain downstream of the step. The mutual influence of multiple walls on the eddy viscosity was taken into account by using an inverse averaging procedure. In the case of two walls, this is done by the following formula:

$$\mu_t = \frac{(\mu_t/n)_1 + (\mu_t/n)_2}{(1/n_1^2 + 1/n_2^2)^{1/2}}$$

where the indices 1 and 2 refer to the two walls.

Pressure distribution along the step-side wall is shown in Fig. 3, resulting from the current approach and from Sindir's calculations using the k–ϵ model. Comparison with the data indicates a slight advantage in using the new algebraic model over the k–ϵ model.

Figure 4 shows the skin friction distribution on the step-side wall. The new backflow model enables improved prediction and significantly better performance in the reattachment zone.

In Fig. 5, streamwise velocity profiles at two locations are shown: one upstream of the reattachment region, the other downstream of it. Agreement with the data is very good at the former location, where the flow is separated, and fair at the latter, where a somewhat premature boundary layer recovery is predicted for the lower part of the profile.

Figure 6 shows Reynolds stress profiles at the locations corresponding to those of Fig. 5. While the shape of the

calculated profile agrees with the experimental one at the upstream location, the magnitude is overpredicted roughly by a factor of two. In the downstream location, however, agreement with data is quite good, although the lower part of the calculated profile is again overpredicted. The location of n_b is also indicated in the figure. Comparing Figs. 5 and 6 leads to the suggestion that while the new model enables good prediction of the time-averaged flowfield, it is not rich enough to enable predicting the gradients thereof, especially away from walls.

Case 2

In Fig. 7, a schematic of the bump flow problem is shown along with a detail of the 80×40 grid, with the first grid line at a distance of 1.0×10^{-5} c off the wall. The boundary conditions used in computing this problem were: freestream at both inflow and upper (farfield) boundaries, nonreflective conditions at the downstream boundary, and no-slip on the surface, which was assumed to be an adiabatic wall.

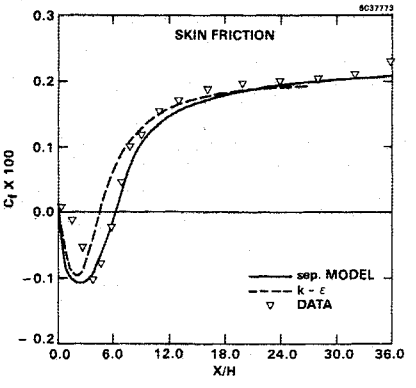

Fig. 4 Step-side skin friction distribution.

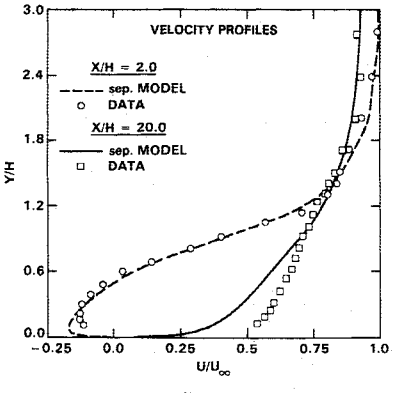

Fig. 5 Streamwise velocity profiles upstream and downstream of reattachment.

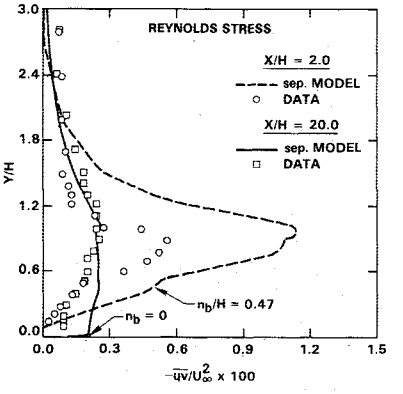

Fig. 6 Reynolds stress profiles corresponding to Fig. 5.

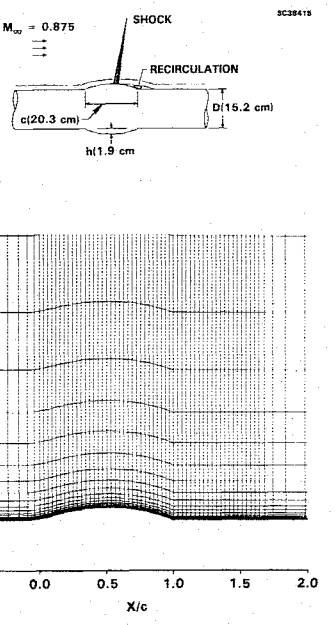

Fig. 7 Schematic and grid detail for the bump problem.

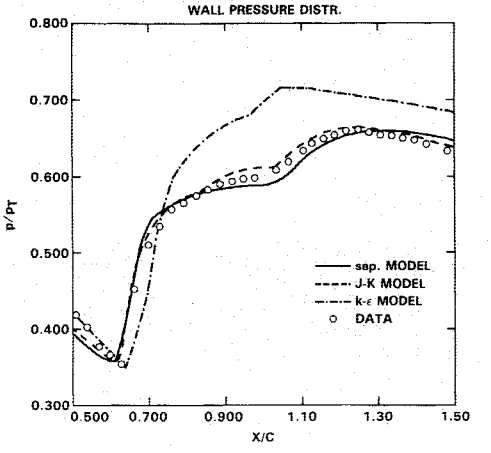

Fig. 8 Wall pressure distribution.

In Fig. 8, wall pressure distribution prediction is compared with experimental data and calculations using a low-turbulence Reynolds number version of the k-ϵ model, as reported in Ref. 3, and the Johnson-King model, reported in Ref. 6. The new turbulence model enables considerably improved agreement with the data, compared to the k-ϵ model, and it performs as well as the Johnson-King model.

Predicted skin friction is compared with the k-ϵ and Johnson-King calculations in Fig. 9. Experimental data for the separation and reattachment points are indicated. Again, the present model performs as well as the Johnson-King model and outperforms the k-ϵ model in predicting the points of separation and reattachment.

Two velocity profiles, at $x/c = 0.875$ and 1.125 are shown in Fig. 10. The agreement with the data is fairly good in view of the fact that the inflow boundary conditions precluded correct boundary layer development along the surface. A profile calculated using the Johnson-King model is shown for $x/c = 0.875$. In Fig. 11, Reynolds shear stress predictions are compared with data at the locations corresponding to those of Fig. 10. Agreement is reasonable. The locations of n_b are also indicated.

Conclusions

A recently introduced algebraic backflow model has been incorporated into a Reynolds-averaged Navier-Stokes solver

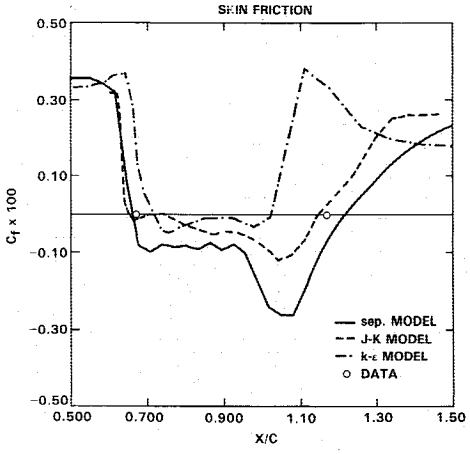

Fig. 9 Skin friction distribution.

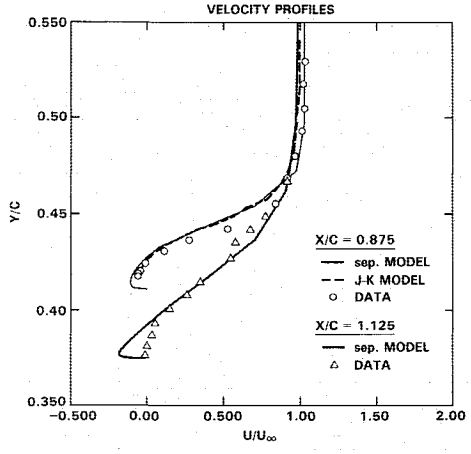

Fig. 10 Velocity profiles at $x/c = 0.875$ and 1.125.

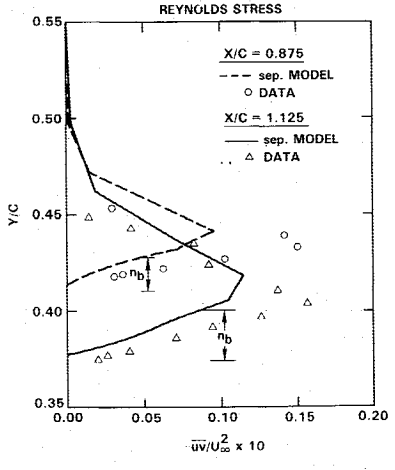

Fig. 11 Reynolds shear stress profiles corresponding to Fig. 10.

that used the Baldwin-Lomax turbulence model outside of separation bubbles. This code has been applied to calculate the reattaching flow over a backward-facing step and the shock-induced separated flow over an axisymmetric bump. Comparisons with data show improvement in predictive capability as compared to that resulting from using the k–ϵ model and a similar performance to that of the Johnson-King model. The new model enables good prediction of time-averaged flow quantities as well as skin friction but falls short of adequately predicting Reynolds shear stresses, although the qualitative prediction of these stresses is good. Since the new model is a simple algebraic one, it should be found attractive for use wherever flow separation is expected.

Appendix

The following algebraic distribution of eddy viscosity is prescribed throughout the backflow region (see Fig. 1 for definitions of the nomenclature):

$$v_t = u_s n_v \sqrt{\rho w/\rho}\, \underbrace{\mathcal{G}^{1/2}(s,n)}_{\text{wake term}} \underbrace{[A(n/n_b)+B]}_{\text{near wall term}} / \underbrace{(2\sqrt{2}\beta^2)}_{\text{low Reynolds number term}},\quad 0 \le n \le n_b$$

where

$$\frac{n_v}{n_b} = 1 + 20\left(\frac{v_w}{u_s n_b}\right) C_\mu^{1/4}$$

$$\mathcal{G}(s,n) = \frac{\rho k}{\rho_b k_b} = [1 - e^{-\phi (n/n_b)^2}]/[1 - e^{-\phi}]$$

$$\beta = k_v/k_b = 1 + [(n_v/n_b)^2 - 1]\,\phi/(e^\phi - 1)$$

$$u_s = \sqrt{(-\overline{uv})_{\max}} = \sqrt{v_{t,m}(\partial U_t/\partial n)_{\max}}$$

$$v_{t,m} = v_t\,|_{\partial U_t/\partial n = \max}$$

with

$$A = -(C_\mu^*/2)^{9/5},\quad B = (C_\mu^*/2)^{3/5} - A,\quad C_\mu = 0.09,$$
$$C_\mu^* = 0.7,\quad \phi = 0.5$$

The development and rationale for this functional form is given in Ref. 7.

For high Reynolds number flows, the above formula for all practical purposes can be reduced to

$$(v_t)_{\text{inner}} = C_1 u_s n_b \sqrt{pw/\rho}\,[A(n/n_b)+B]\sqrt{\mathcal{G}(s,n)},\quad 0 \le n \le n_b$$

$$(v_t)_{\text{outer}} = C_2 u_s n_b \sqrt{pw/\rho},\quad n > n_b$$

$$C_1 \approx 0.353,\quad C_2 \approx 0.188$$

References

[1]Driver, D.M. and Seegmiller, H.L., "Features of a Reattaching Turbulent Shear Layer in Divergent Channel Flow," *AIAA Journal,* Vol. 23, Feb. 1985, pp. 163–171.

[2]Sindir, M., "Numerical Study of Separating and Reattaching Flows in a Backward-Facing Step Geometry," Ph.D. Dissertation, Mechanical Engineering, Univ. of California at Davis, CA, 1982.

[3]Sahu, J. and Danberg, J.E., "Navier-Stokes Computations of Transonic Flows with a Two-Equation Turbulence Model," *AIAA Journal,* Vol. 24, Nov. 1986, pp. 1744–1751.

[4]Goldberg, U.C., "Separated Flow Calculations with a New Turbulence Model," presented at the IACM First World Congress on Computational Mechanics, Austin, Texas, Sept. 1986.

[5]Bachalo, W.D. and Johnson, D.A., "An Investigation of Transonic Turbulent Boundary Layer Separation Generated on an Axisymmetric Flow Model," AIAA Paper 79-1479, 1979.

[6]Johnson, D.A. and King, L.S., "A Mathematically Simple Turbulence Closure Model for Attached and Separated Turbulent Boundary Layers," *AIAA Journal,* Vol. 23, Nov. 1985, pp. 1684–1692.

[7]Goldberg, U.C., "Separated Flow Treatment with a New Turbulence Model," *AIAA Journal,* Vol. 24, October 1986, pp. 1711–1713.

[8]Chakravarthy, S.R., Szema, K.-Y., Goldberg, U.C., Gorski, J.J., and Osher, S., "Application of a New Class of High Accuracy TVD Schemes to the Navier-Stokes Equations," AIAA Paper 85-0165, Jan. 1985.

[9]Chakravarthy, S.R., "The Versatility and Reliability of Euler Solvers based on High-Accuracy TVD Formulations," AIAA Paper No. 86-0243, Jan. 1986.